

## Shear Reinforcement with Glass Fibre Polymer in Reinforced Concrete Beams

Sabrina Lopes Arcenego<sup>1</sup>, Sarah Lodeti Pessi<sup>2</sup>, Augusto Wanderlind<sup>3</sup>,  
Jorge Henrique Piva<sup>4</sup>, Elaine Guglielmi Pavei Antunes<sup>5</sup>

<sup>1</sup>Structural and Construction Performance Research Group, Department of Civil Engineering, University of the Southern Santa Catarina, University Avenue, 1105 - University District, 88806-000, Criciúma, Santa Catarina, Brazil ([sabrinaarcenego@hotmail.com](mailto:sabrinaarcenego@hotmail.com)) ORCID [0000-0002-0006-9388](https://orcid.org/0000-0002-0006-9388);

<sup>2</sup>Structural and Construction Performance Research Group, Department of Civil Engineering, University of the Southern Santa Catarina, University Avenue, 1105 - University District, 88806-000, Criciúma, Santa Catarina, Brazil ([sara.lodeti@hotmail.com](mailto:sara.lodeti@hotmail.com)) ORCID [0000-0002-3085-9575](https://orcid.org/0000-0002-3085-9575);

<sup>3</sup>Structural and Construction Performance Research Group, Department of Civil Engineering, University of the Southern Santa Catarina, University Avenue, 1105 - University District, 88806-000, Criciúma, Santa Catarina, Brazil ([acw@unescc.net](mailto:acw@unescc.net)) ORCID [0000-0002-5312-9700](https://orcid.org/0000-0002-5312-9700);




<sup>4</sup>Structural and Construction Performance Research Group, Department of Civil Engineering, University of the Southern Santa Catarina, University Avenue, 1105 - University District, 88806-000, Criciúma, Santa Catarina, Brazil ([jhpiva@gmail.com](mailto:jhpiva@gmail.com)) ORCID [0000-0002-1753-4944](https://orcid.org/0000-0002-1753-4944); <sup>5</sup>Structural and Construction Performance Research Group, Department of Civil Engineering, University of the Southern Santa Catarina, University Avenue, 1105 - University District, 88806-000, Criciúma, Santa Catarina, Brazil ([elainegpa@unescc.net](mailto:elainegpa@unescc.net)) ORCID [0000-0002-9698-1100](https://orcid.org/0000-0002-9698-1100)

### Abstract

Reinforcement of a structure is necessary in unpredictable changes or also for rehabilitation, due to exposure to weather conditions, causing considerable damage that can lead to the collapse of the structure. The present study aims to evaluate the behavior of the strengthening with sheets of glass fiber reinforced polymer (GFRP) with thicknesses of 3 mm, bonded with structural epoxy-based adhesive applied in the shear area of reinforced concrete beams, spaced in three different configurations and bonded on the two faces of the beam. The beams were cracked previously to simulate a damaged structure and strengthened later to obtain the maximum load of rupture after the application of the strengthening. With the obtained results it can be verified an increase of ductility in the reinforced concrete beams. The increase of the load capacity was obtained in the beams with strengthening with smaller spacing between the sheets.

**Author Keywords.** Pathologies, GFRP, Concrete, Shear.

**Type:** Research Article

 Open Access  Peer Reviewed  CC BY

### 1. Introduction

The need for fast execution in a short period of time makes the demand for new construction methods grow and, therefore, the insertion of new technologies and innovations has been stimulating the modernization of the civil engineering sector. In this context new materials also stand out, more technological and allowing greater efficiency, such as the pultruded profile structures.

Glass fiber reinforced polymer (GFRP) is widely used due to its advantages, having a relatively light core, high mechanical strength and non-corrosive properties (Koaik, Bel, and Jurkiewicz 2017; Zhang et al. 2019). Moreover, after the composite is formed, it exhibits orthotropic properties, i.e., it has its mechanical properties changed according to the loading direction. When the load is applied in the direction of the fibers, the compressive strength equals the

tensile strength. Considering the transverse loading, the compressive strength is greater than the tensile strength (Zhang et al. 2020).

When it comes to conventional structures of reinforced concrete, it is known that the structure presents difficulties with respect to unforeseen structural changes, in addition to the structure is also imposed to environmental conditions of weathering causing considerable damage, which can cause pathologies or even the collapse of the structure (Hadigheh and Kashi 2018).

As a means of increasing the strength of the structure, one of the methods used is bonding steel plates or fiber composites (FRP) to the surface of the beam (Kalfat et al. 2018). Several studies, such as those conducted by Khalifa and Nanni (2002), Adhikary and Mutsuyoshi (2004) and Pellegrino and Modena (2006), have shown that the application of FRP in RC beams increases the overall shear capacity of a structural member.

Usually GFRP, CFRP or FRP plates are applied as reinforcement in all faces of the structural element, being more commonly employed for flexural reinforcement, but it is easier to detach (Mugahed Amran et al. 2018). When applied externally on the lateral faces in strip format, it causes better performance to vertical shear stress, vertical, inclined, laterally bonded, U-wrapped or anchored configurations can be applied (Chen et al. 2017; Siddika et al. 2019). It is noteworthy that when a beam presents deficiency to shear, the failure may occur suddenly without previous warning, because it is of fragile nature. Thus, deficiencies in shear strength demand more attention than bending failures, which are ductile in nature (Panda, Bhattacharyya, and Barai 2011; Akroush et al. 2017). In a comparative study of various types of FRP strengthening in the shear area, it was observed an increase in the shear capacity of the beams studied, especially when anchorage was used. It was also observed change of failure mode from shear to bending (Baggio, Soudki, and Noël 2014). Among all the reinforcement systems, the system with inclined strips was considered as the most effective technique for increasing the shear capacity (Siddika et al. 2020; Sim et al. 2005). About 11,9% and 7,7% increase in load capacity were observed after wrapping a RC beam with a 45° oriented CFRP sheet and a bidirectional CFRP sheet, respectively (Singh 2013).

CFRP strengthening was also applied to repair shear cracks developed in a damaged beam by externally applying a prestressing force, which resulted in a 57,0% increase in load carrying capacity (Hussein, Afefy, and Khalil 2013). It was proved that, the ultimate shear capacity of the strengthened beam can be effectively increased by 82,2%, when no internal stirrup used in the critical shear area (Ebead and Saeed 2017).

The literature also shows research studies, comparing experimental data with analytical models of reinforced concrete beams with externally bonded FRP as shear reinforcement (Chen and Teng 2003). Among these models applied in the prediction of load capacity, the one developed by Triantafillou and Antonopoulos (2000) and the ACI 440 2R-08 (American Concrete Institute 2015) model, the former shows to be more suitable for the conservative design of fully wrapped rectangular beams, while the prediction for T-beams and some rectangular beams, with smaller reinforcement area, is not safe (Ary and Kang 2012).

Most studies are dedicated to the strengthening of beams with reduced design to shear force, so as a contribution to research, it is proposed to evaluate pre-damaged beams in the shear region.

Given the above, the objective of this work is to analyze the mechanical behavior of pre-cracked reinforced concrete beams strengthened with pultruded material, bonded with epoxy resin in the shear region, in three different spacing configurations.

## 2. Materials and Methods

The research was divided into two phases, and in the first, a four-point bending test was performed on three pilot beams in order to verify the maximum load that these beams could support until failure. This information determines the force that is applied to the rest of the beams, which led to the appearance of visible cracking. It was chosen to apply a pre-load until the visible cracking, in an attempt to make the damage caused similar to a real condition of use. This damage caused in the beams aims to represent possible real failures that could happen in practice. It is worth noting that the objective is to analyze cracked and unbroken beams to study the behavior considering the repair.

The second phase corresponds to the strengthening of the cracked beams, using sheets of structural polymer pultruded with epoxy resin (GFRP), with dimensions of 5,0 cm wide and 20,0 cm high with a thickness of 3,0 mm. The sheets were bonded with epoxy resin on both faces of the shear area of the beam. The referred beams were tested again so that their load after the structural strengthening was analyzed.

### 2.1. Beam dimensioning routine

The compressive strength defined for the concrete was 20 MPa ( $f_{ck}$ ), a minimum strength condition for structural elements. These parameters are established by ABNT NBR 6118 (ABNT 2014), item 7.1. Which states that for this concrete strength, it must respect environments with aggressiveness class I, i.e., corresponding to a weak aggressiveness, with negligible risk of deterioration by environmental agents. According to the class of aggressiveness and quality of the concrete, the cover for the reinforcement must be 25 mm.

The beams were dimensioned with cross sections of 12,0 cm wide, 20,0 cm high and 190,0 cm long. Based on the characteristics of the beam cross section and the materials used, the section was modeled in strain domain 2, with ratio  $x/d = 0,24$ . The neutral axis depth ( $x$ ) for the ultimate limit state (ULS), was determined by Formula (1), according to the recommendations of NBR 6118 (ABNT 2014), considering the equilibrium of the tensile forces in the reinforcement and compression in the concrete.

In this work, the equations used, for concrete and steel, characteristic values were adopted, not design values. The tests were conducted under controlled laboratory conditions, avoiding possible unfavorable deviations of the materials in the structure from the characteristic values and possible geometric inaccuracies. Therefore, the strength reduction coefficients of steel and concrete,  $\gamma_s$  and  $\gamma_c = 1$ .

$$x = \frac{A_s \cdot (f_{yk}/\gamma_s)}{b_w \cdot (f_{ck}/\gamma_c) \cdot \lambda} \quad (1)$$

Where:

$x$  – depth of the neutral line, measured from the edge of the most compressed edge, (cm);  
 $A_s$ – total steel area of the main longitudinal reinforcements, (cm<sup>2</sup>);  $b_w$  – width of the cross section of the rectangular beams, (cm);  $f_{yk}$  – characteristic yield strength steel, with  $f_{yk} = 500$  MPa;  $f_{ck}$  – characteristic compressive strength of concrete, with  $f_{ck} = 20$  MPa;  $\gamma_s = 1,0$ ;  $\gamma_c = 1,0$ ;

$\lambda$  – coefficient of approximation of the stress distribution of compressed concrete for equivalent rectangle.  $\lambda = 0,80$  for  $f_{ck} \leq 50$  MPa.

The theoretical ultimate resisting moment for the reinforced concrete beams was determined by Formula (2), which takes into account the acting force in the longitudinal reinforcement and the neutral axis depth in the ULS.

$$M_u = (f_{yk}/\gamma_s) \cdot A_s \cdot (d - 0,4x) \quad (2)$$

Where:

$M_u$  – last resistant moment foreseen for the beam in the ULS, (kN.m);  $A_s$ – total steel area of the main longitudinal reinforcements, (cm<sup>2</sup>);  $d$  – useful beam height, (cm);  $x$  – depth of the neutral line, measured from the edge of the most compressed edge, (cm);  $f_{yk}$  – characteristic yield strength steel, (MPa);  $\gamma_s$  – coefficient for the reduction of steel resistances. In this work  $\gamma_s = 1,0$ .

Based on equation 2, the beams are able to support a characteristic bending moment  $M_k = 12,0$  kN.m. Figure 1 presents the loads applied in the four-point bending test to which corresponds the bending moment. The loads coming from the own weight of the beams were unconsidered.

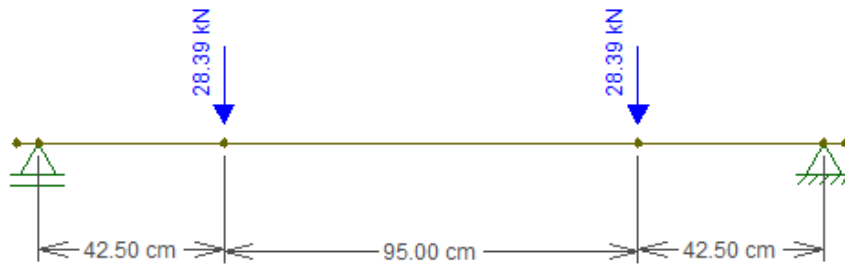


Figure 1: Loads considered in the beams

The steel used was CA-50 ribbed, with yield stress and longitudinal modulus of elasticity of  $f_y = 500$  MPa and  $E_s = 210$  GPa, respectively. It was adopted two steel bars with 10 mm diameter for flexural reinforcement ( $A_s = 1,6$  cm<sup>2</sup>) and two bars with 5 mm diameter for stirrup holders, according to the criteria of NBR 6118 (ABNT 2014).

The transverse reinforcement was dimensioned adopting calculation model I, with stirrups vertically ( $\alpha = 90^\circ$ ) according to the methodology of NBR 6118 (ABNT 2014). All calculations were performed considering that the transverse reinforcement was composed by simple branches with ribbed CA-50 steel bars of 5 mm diameter. For the characteristics of the beam under study, applying the standard methodology, the spacing between the stirrups resulted in 30,0 cm, totaling 06 stirrups for each beam. Figure 2 shows the detailing of the reinforcement in the beam, Figure 2(a) shows the longitudinal detailing and Figure 2(b) the frame perspective.

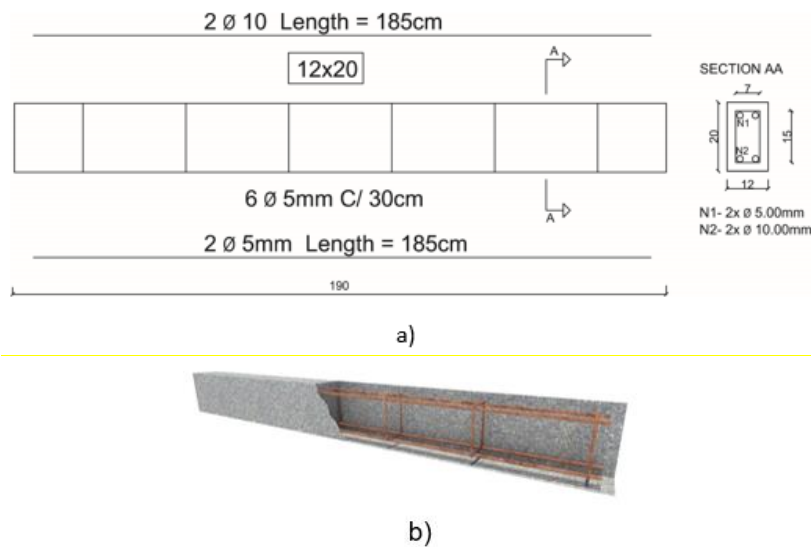


Figure 2: Detailing of the reinforcement in the beams - (a) Longitudinal detailing; (b) Frame perspective

## 2.2. Materials characterization

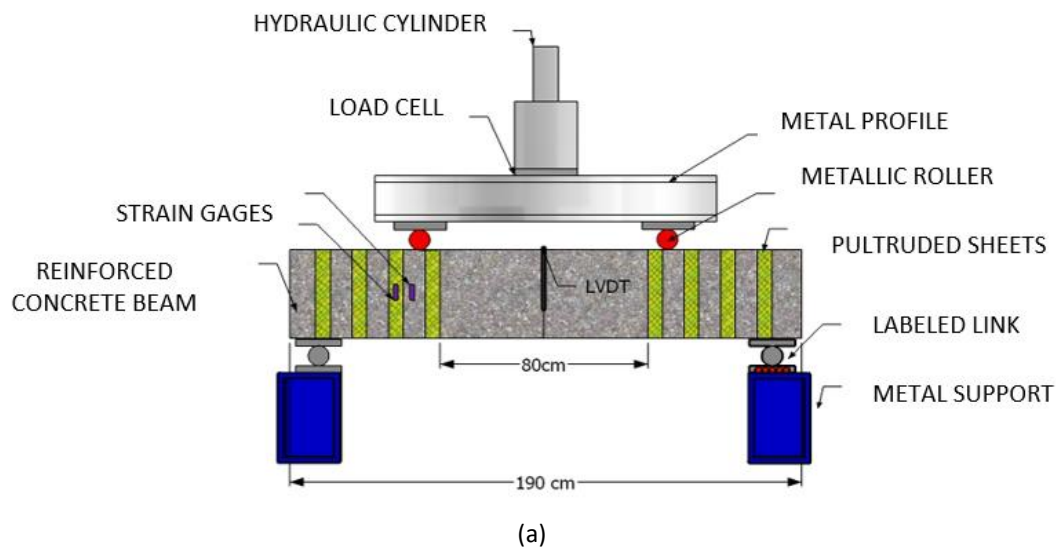
For the technological control of the concrete, the fresh concrete was characterized through the slump test, according to NBR NM 67 (ABNT 1998), which resulted in 10 cm.

Fifteen cylindrical specimens were cast according to NBR 5738 (ABNT 2015), parallel to the concreting of the beams, in order to obtain the axial compressive strength of concrete at 28 and 56 days. For complementary purposes, at 56 days, the modulus of elasticity and diametral compression tests were performed, according to NBR 8522 (ABNT 2017) and NBR 7222 (ABNT 2011), respectively. After concreting, the beams were cured for 56 days and then the tests were performed.

## 2.3. Experimental test

Of the total of fifteen beams concreted, three of them were tested until failure. The analysis of rupture of a beam imposed to shear forces according to Araújo (2014), when the beam is without cracking, it is in stage I and when the principal stress reaches the tensile strength of concrete, an inclined crack appears and the beam enters the stage II. When the structure presents excessive deformation limits and a level of cracking that compromises the durability, exceeding its serviceability limit state, it is considered its rupture. The failure mode of the reference beams was established from the beginning of the load drop where the concrete rupture occurs and consequently the load loss gradually. The remaining twelve beams were tested until they presented visible cracking, consequently, stage II, aiming to be above the indicated limits, leading to cracking of the concrete among other anomalies.

The beams were subjected to the static bending test at four points. A metallic frame was used and the load was applied by means of a hydraulic press with capacity of maximum reading of 500kN and a load cell coupled to its base. To obtain the maximum displacement of the beams, a displacement transducer (LVDT) was used with a maximum reading of 100 mm, located at the center of the beam span. All the equipment is connected to the Quantum X<sup>®</sup> data acquisition system that uses Catman Easy<sup>®</sup> software, both from HBM<sup>®</sup>. For a better analysis, two strain gages were installed in each group of beams, one at the concrete interface and the other at the strengthening plate. Figure 3 shows the test scheme, Figure 3(a) the shear force and Figure 3(b) bending moment diagram, according to NBR 6118 (ABNT 2014), thus justifying the application of the strengthening in the shear area of the beam.



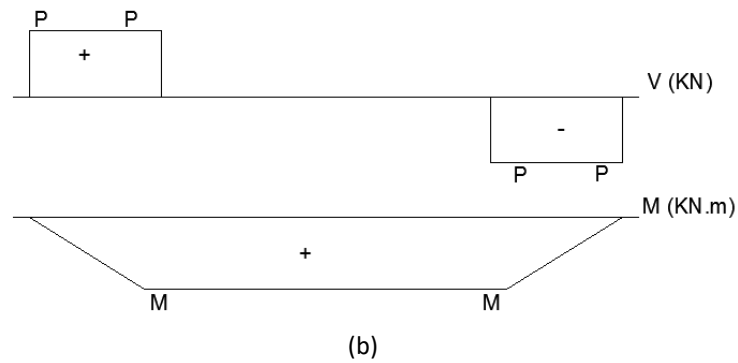


**Figure 3:** (a) Schematic of the static bending test at four points; (b) Shear force and Bending Moment Diagram

### 2.4. Structural reinforcement process

The standard ACI 440 2R-08 (American Concrete Institute 2015) provides for three types of FRP wrapping schemes, used to increase the shear strength of prismatic and rectangular beams, completely wrapping the FRP system around the section, 3-sided and 2-sided beam wrapping. In all wrapping schemes, the FRP system can be installed continuously along the span of a member or placed as discrete strips. In this work, the configuration with the least use of material was adopted, that is, on two sides and in strips.

The twelve beams cracked in the previous step, were used for bonding of the structural polymer plates pultruded with epoxy resin (GFRP). For analysis of the strengthening, three configurations of different spacing between the reinforcements were used. Each Group was composed of four beams. The first configuration is the Group 100, with plates spaced every 10,0 cm totaling 16 plates, the second configuration is the Group 175, with plates spaced every 17,5 cm totaling 12 and the last configuration to be analyzed is the Group 400, with plates with spacing of 40,0 cm totaling 8 plates, as shown in Figure 4.

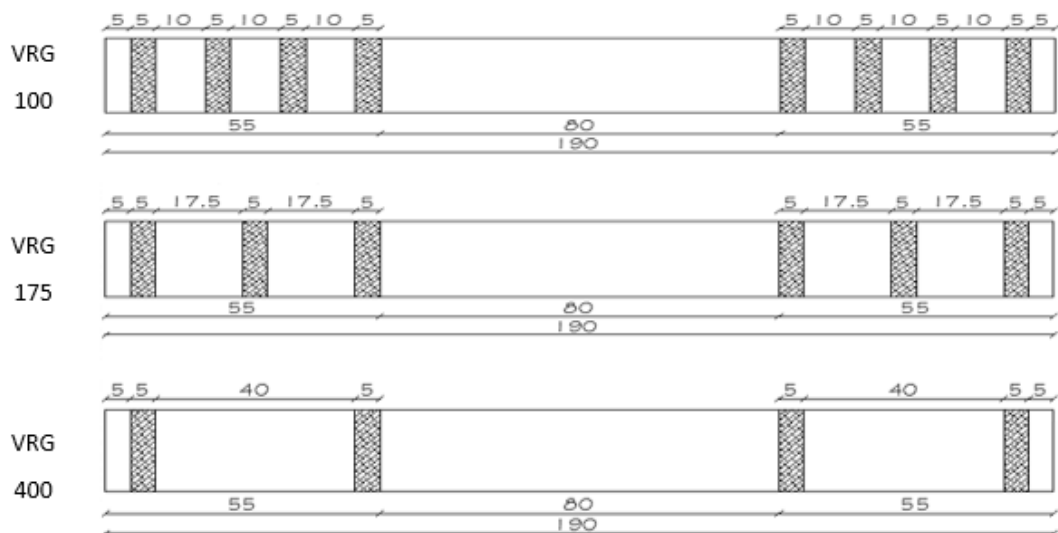


**Figure 4:** Detailing of reinforcements for the three groups with their respective spacing

The GFRP sheets used as reinforcement were 3 mm thick, 50 mm wide and 200 mm long. The mechanical properties adopted for the GFRP reinforcement were based on the study conducted by Hoffman et al. (2020), being longitudinal modulus of elasticity ( $E_f = 21,36$  GPa), tensile strength ( $f_{fu} = 265,00$  MPa) and strain at break ( $\epsilon_{fu} = 0,011$ ).

The structural adhesive used is a chemical compound based on epoxy resin, high viscosity, solvent free, composed by aggregate properly dosed and normal setting. It denotes as spare

characteristics a high adhesion power, high performance in structural repair and strengthening of concrete structures, contains pre-dosed material and presents initial hardness in 24 hours after being applied, and total cure 7 days after the application of the product on the beam. For the application of the structural adhesive, the surface was properly cleaned, free of dust, release agents, oils or any other type of contaminating material and the reinforcement plates were also manually sanded for better adherence. The epoxy-based structural adhesive was applied with a maximum thickness of 2,0 mm and with the aid of spatulas. After the resin curing time, the beams were tested again and taken to failure to then obtain the maximum load value after the structural strengthening.

#### 2.4.1. Theoretical study

The approach proposed by ACI 440 2R-08 Guide for the Design and Construction of Externally Bonded FRP Systems for Strengthening Concrete Structures ([American Concrete Institute 2015](#)) is adopted to reinforced concrete beams with externally applied GFRP strengthening. According to this standard, the shear strength of a GFRP-reinforced concrete member can be determined by adding the contribution of the reinforcement to the contribution of steel and concrete.

The standard has recommendations and analytical formulas capable of quantifying these reinforcements.

Following the standard ACI 440 2R-08 ([American Concrete Institute 2015](#)), the shear strength can be calculated with [Formula \(3\)](#).

$$\phi V_n = \phi(V_c + V_s + \phi_f V_f) \quad (3)$$

Where:

$\phi$ - lessening resistance factor;  $V_n$ - nominal shear strength, (N);  $V_c$ - shear strength referring to concrete, (N);  $V_s$ - shear strength referring to steel, (N);  $\phi_f$ - coefficient of reduction of reinforcement efficiency;  $V_f$ - shear strength referring to reinforcement, (N).

For the study of this work the factor  $\phi$  was adopted as 1,0, in order to compare with the experimental responses, the reduction factor  $\psi$  of 0,85 is recommended for U-shaped reinforcement schemes of three-sided FRP or two-sided opponent. The resistances  $V_c$  and  $V_s$  were calculated with [Formula \(4\)](#) and [Formula \(5\)](#), taken from the American standard ACI 318-05 Building Code Requirements for Structural Concrete and Commentary ([American Concrete Institute 2005](#)).

$$V_c = 2\sqrt{f'_c} b_w d \quad (4)$$

$$V_s = \frac{A_v f_{yt} d}{s} \quad (5)$$

Where:

$f'_c$  - characteristic compressive strength of concrete, (psi);  $b_w$  - width of the cross section of the concrete beam, (mm);  $d$  - distance from the most compressed face to the centroid of the longitudinal steel reinforcement, (mm);  $A_v$  - area of steel transverse reinforcement with spacing  $s$ , (mm<sup>2</sup>);  $f_{yt}$  - yield strength of the transverse reinforcement, (MPa);  $s$  - spacing between transverse reinforcements, (mm).

In [Formula \(4\)](#) the psi unit should be used for  $f'_c$ . The other equations in the article are adapted to use the units of the international system.

The equation to obtain the resistance  $V_f$  that appears in the referred standard is based on spaced stiffeners. For its calculation, [Formula \(6\)](#) and [Formula \(7\)](#) are used.

$$V_f = A_{fv}f_{fe} \quad (6)$$

$$A_{fv} = 2nt_fw_f \quad (7)$$

Where:

$A_{fv}$  - shear reinforcement area from GFRP, (mm<sup>2</sup>);  $f_{fe}$  - effective tensile strength of GFRP, (MPa);  $t_f$  - nominal thickness of one ply of GFRP reinforcement, (mm);  $w_f$  - width of GFRP reinforcing plies, (mm).

To obtain  $f_{fe}$  acting against shear, the linear relationship by Hooke's law can be used, but an effective deformation ( $\varepsilon_{fe}$ ) must be considered, which experimentally obtains values lower than those of concrete fracture, characterising a fracture by disconnection of the reinforcement with the concrete (Mugahed Amran et al. 2020).

Formula (8), (9), (10), (11), (12) and (13) lead to characterise the shear behavior of the reinforcement until ( $\varepsilon_{fe}$ ) is obtained, which is a function of concrete strength, reinforcement cross section and reinforcement stiffness (Khalifa et al. 1998).

$$\varepsilon_{fe} = k_v\varepsilon_{fu} \quad (8)$$

$$k_v = \frac{k_1k_2L_e}{11900\varepsilon_{fu}} \quad (9)$$

$$k_1 = \left(\frac{f'_c}{27}\right)^{2/3} \quad (10)$$

$$k_2 = \frac{d_{fv} - 2L_e}{d_{fv}} \quad (11)$$

$$L_e = \frac{23300}{(n_ft_fE_f)^{0,58}} \quad (12)$$

$$f_{fe} = E_f\varepsilon_{fe} \quad (13)$$

Where:

$k_v$  - reduction coefficient of the shear deformation efficiency;  $\varepsilon_{fu}$  - limit deformation for rupture of the GFRP, (mm/mm);  $k_1$  - reduction factor due to the influence of concrete strength;  $k_2$  - reduction factor due to the influence of the reinforcement for two sides bonded;  $d_{fv}$  - web height of the collaborative form of GFRP, (mm);  $n_f$  - modular ratio of elasticity between GFRP and concrete =  $E_f/E_c$ ;  $E_f$  - longitudinal elastic modulus of the GFRP, (MPa);  $L_e$  - active length of the connection of the GFRP with the concrete over which most of the shear tension is maintained, (mm).

### 3. Results and Discussions

The compressive strength test was performed after 28 days of curing of the specimens, and afterwards and parallel to the beam tests, the remaining specimens were also tested for modulus of elasticity and diametral compression at 56 days. Table 1 shows the results of these tests.



Ages of the specimens(days)	Compressive Strength (MPa)	Tensile strength by diametral compression (MPa)	Modulus of Elasticity (MPa)
28	21,3	-	-
28	22,2	-	-
28	20,3	-	-
Average (S.D)	21,3 (±0,9)		
56	26,0	11,3	28,9
56	26,2	11,9	30,4
56	26,6	12,9	26,6
Average (S.D)	26,3 (±0,3)	12,0 (±0,8)	28,6 (± 2,7)

**Table 1:** Results of Compressive Strength, diametral compression strength and modulus of elasticity

The average compressive strength at 28 and 56 days of curing reached 21,3 MPa and 26,3 MPa, respectively, which represents a performance above the minimum strength required by standard NBR 6118 (ABNT 2014), which is 20 MPa.

### 3.1. Results of the flexural tests on the beams

The expected result of the reference beams, through NBR 6118 (ABNT 2014), was a theoretical load capacity of 56,8 kN for shear. For the beams the maximum vertical displacement should be obtained through its length divided by 250 (L/250), NBR 6118 (ABNT 2014), presents the limit values that aim to provide an adequate behavior of the structure in service, so the maximum vertical displacement for the beams under study was 7,2 mm. Table 2 presents the results obtained for the reference beams.

VREF (reference beams)	Rupture Load (kN)	Displacement (mm) L/250 = 7,2 mm
1	53,0	10,5
2	52,3	10,0
3	50,7	9,4
Average	52,0	10,0
S. D.	1,2	0,5

**Table 2:** Results of ruptured reference beams

Based on Table 2 it can be verified that the beams behaved as expected. The failure of all beams occurred by shear stress with an inclined shear crack of approximately 45° and the average maximum load of rupture was 52,0 kN. Figure 5 presents the reference beams after the rupture, Figure 5(a) being VREF 01, Figure 5(b) VREF 02 and Figure 5(c) VREF 03.

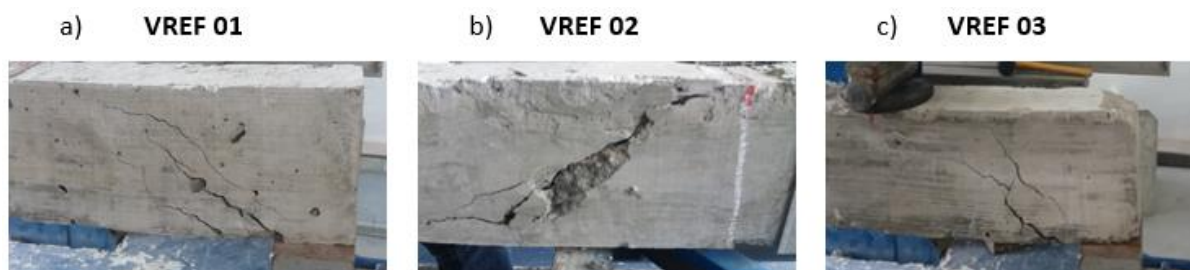


**Figure 5:** Reference beams after the test; (a) VREF 01, (b) VREF 02 and (c) VREF 03

After determining the failure load of the reference beams, the remaining twelve beams were taken to the first test stage, where each beam was monitored until its visible cracking. In this

first stage all beams presented shear cracking as expected, Figure 6 presents the cracked beams, Figure 6(a) being VGR 100, Figure 6(b) VGR 175 and Figure 6(c) VGR 400.

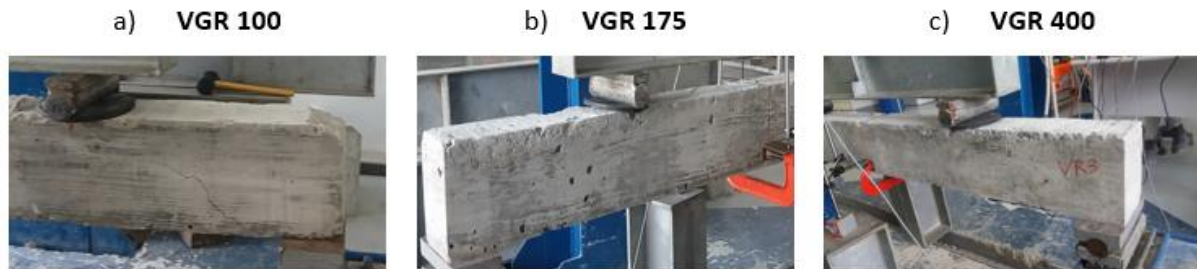


Figure 6: Beams after testing for pre-cracking: a) VGR 100, b) VGR 175, and c) VGR 400

Table 3 presents the results of the flexural test on the beams before and after strengthening with GFRP. Using the experimental results obtained, a comparison between these results and those predicted by the model of ACI 440 2R-08 (American Concrete Institute 2015) was performed. Once these formulations were developed for strengthened beams without cracks, it was verified the application of the model in the repaired beams with cracks caused previously, this way the theoretical concrete strength ( $V_{c,theor}$ ) was considered equal to zero.

specimen	Before strengthening					After strengthening					
	Beam	Load theoretic (kN)	$V_{theor}$ (kN)	Load at failure (kN)	$V_{test}$ (kN)	Load at failure (kN)	$V_{n,test}$ (kN)	$V_{f,theor}$ (kN)	$V_{c,theor}$ (kN)	$V_{s,theor}$ (kN)	$\phi V_{n,theor}$ (kN)
VGR 100	1	56,8	28,4	51,8	25,9	51,4	25,7	29,0	0	11,1	35,8
	2	56,8	28,4	44,4	22,2	56,9	28,4	29,0	0	11,1	35,8
	3	56,8	28,4	55,3	27,6	65,6	32,8	29,0	0	11,1	35,8
	4	56,8	28,4	52,6	26,3	67,6	33,8	29,0	0	11,1	35,8
Average		56,8	28,4	51,0	25,5	60,4	30,2	29,0		11,1	35,8
VGR 175	1	56,8	28,4	54,3	27,2	38,3	19,2	19,3	0	11,1	27,6
	2	56,8	28,4	57,0	28,5	65,1	32,5	19,3	0	11,1	27,6
	3	56,8	28,4	53,2	26,6	61,7	30,8	19,3	0	11,1	27,6
	4	56,8	28,4	52,9	26,5	60,3	30,2	19,3	0	11,1	27,6
Average		56,8	28,4	54,4	27,2	56,3	28,2	19,3		11,1	27,6
VGR 400	1	56,8	28,4	48,8	24,4	37,7	18,8	9,7	0	11,1	19,3
	2	56,8	28,4	50,2	25,1	20,4	10,2	9,7	0	11,1	19,3
	3	56,8	28,4	48,8	24,4	66,5	33,3	9,7	0	11,1	19,3
	4	56,8	28,4	53,3	26,6	55,4	27,7	9,7	0	11,1	19,3
Average		56,8	28,4	50,3	25,1	45,0	22,5	9,7		11,1	19,3

Table 3: Comparison of experimental and theoretical results predicted

The increase in load capacity was significant in the strengthened beams, especially with eight GFRP sheets (VGR100), when compared to those with four sheets (VGR400). It can be observed that in groups VGR 100 and VGR 175, there was an increase of the initial load, of 18, 3 % and 3,6 %, respectively. In some cases, as in VGR 175-1, the strengthening did not overlap all cracks, causing a lower failure load than the others. This condition was also observed in beams from VGR 400 group, where the strengthening sheets were insufficient, which resulted in 89,00 % of the load resisted before strengthening.

In the group with the largest number of layers of reinforcement, the tests did not reach the strength predicted by the theoretical model, while for the others, the experimental results showed some consistency with the analytical values of ACI 440.2R-08.

Although the results of this research are still incipient, it can be verified that the load increment of beams repaired by bonding GFRP, with spacings of 10 and 17.5 cm (VGR 100 and VGR 175), were promising and, therefore, after the continuity of the study with applicability, for example, in buildings with deteriorated structures (Bielak et al. 2022).

The deterioration of reinforced concrete structures depends on several factors, such as, the quality of the concrete, the constituents, the design of the concrete mixture, as well as the structure, the site, the supervision and quality of execution, the influence of the environment and, finally, the maintenance (Chemrouk 2015).

Figure 7 demonstrates the strengthened and ruptured beams of groups, Figure 7(a) being VGR 100, Figure 7(b) VGR 175 and Figure 7(c) VGR 400.



Figure 7: Rupture of beams of groups: a) VGR 100; b) VGR 175 and c) VGR 400

### 3.2. Analysis of the displacement results

The results of the displacements of the three groups of strengthened beams were compared with that obtained in the VREF beam and are presented in the next figures; Figure 8, displacements of the VGR 100 group; Figure 9, VGR 175 group and Figure 10, VGR 400 group.

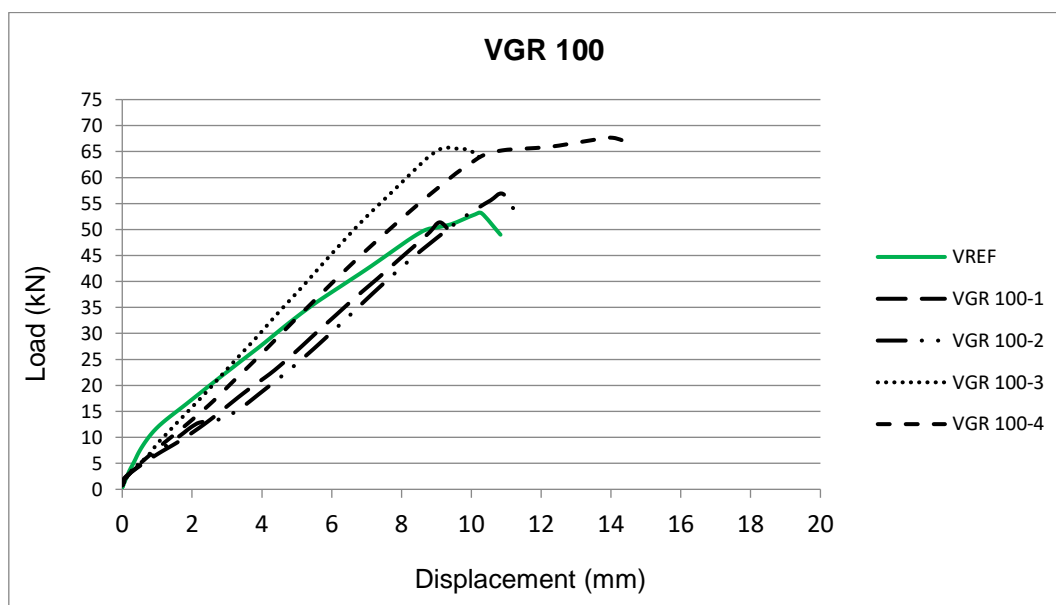


Figure 8: Graph Load x Displacement - VGR 100, after strengthening

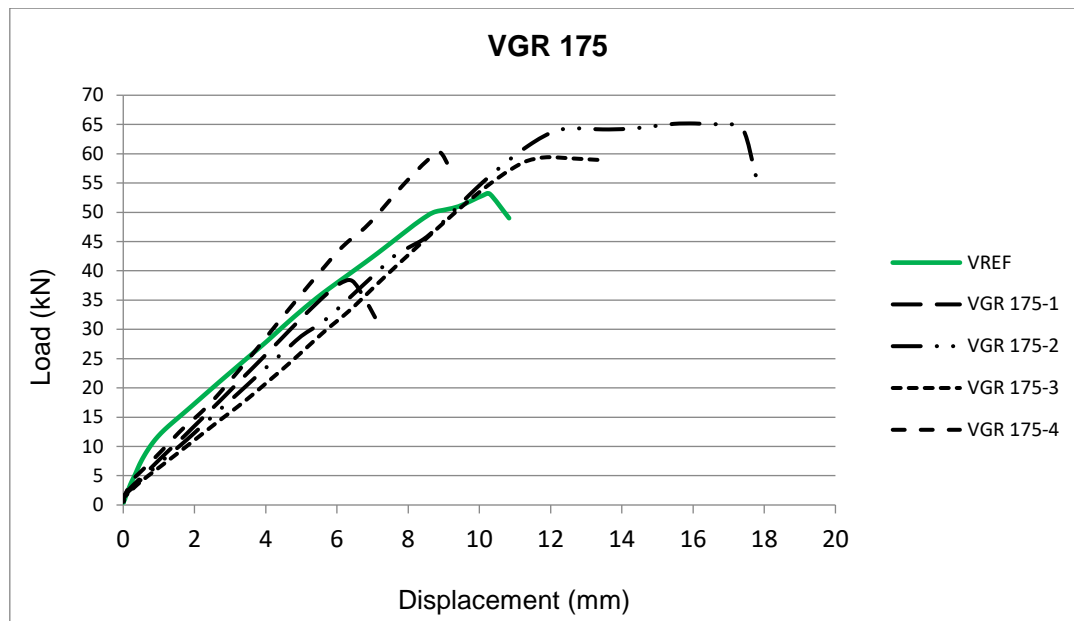


Figure 9: Graph Load x Displacement - VGR 175, after strengthening

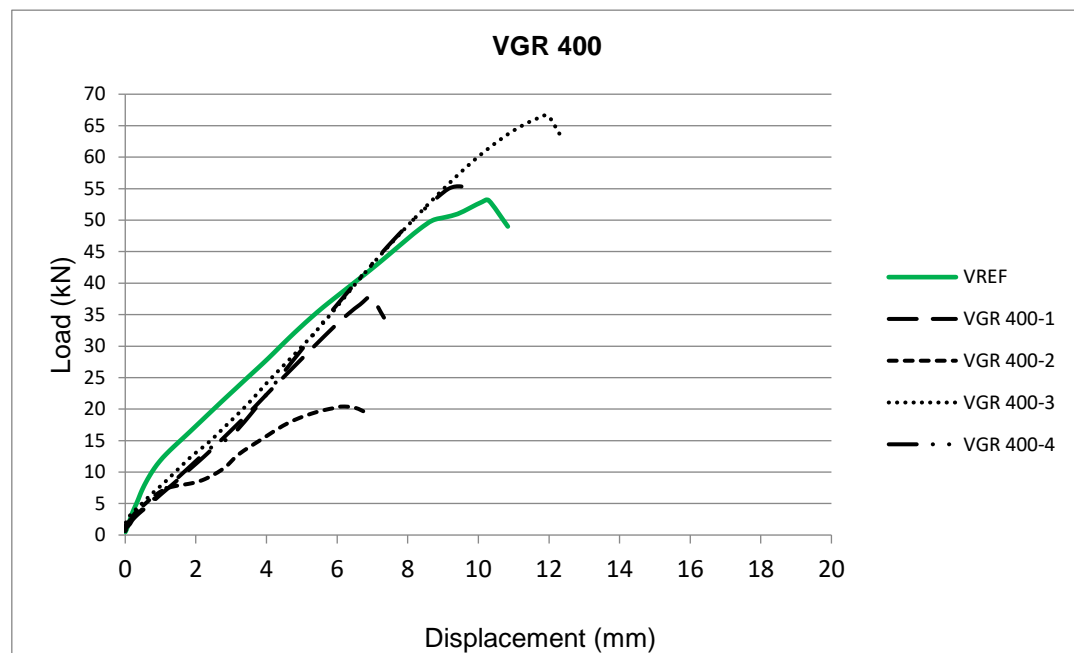


Figure 10: Graph Load x Displacement - VGR 400, after strengthening

The displacement results of the beams show in general an improvement in performance, i.e., higher loads and displacements were reached before failure, which represents an increase in ductility. In the group VGR 100 there is greater uniformity between the results of the four beams, while for the other spacings, VGR 175 and VGR 400 a loss of uniformity is observed. This behavior is noticed mainly in beams from VGR 175 group, the average displacement was higher, but with high amplitude between the lowest and the highest value obtained, due to the fact that the strengthening in some cases coincided its position on the crack, stabilizing it and consequently increasing ductility. According to the analysis of [Baggio, Soudki, and Noël \(2014\)](#) this behavior of ductility increment was also observed in all the experiments conducted. In the VGR 400 group, the strengthening for having a larger spacing, became even less efficient, presenting results below the values of the reference beam.

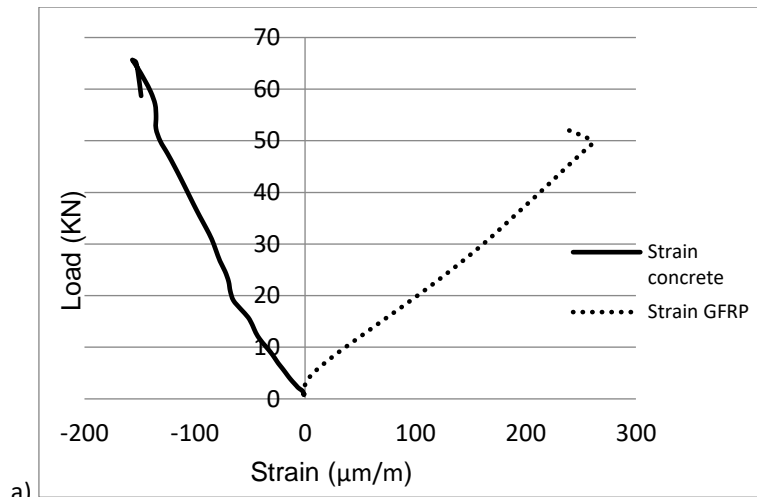
### 3.3. Analysis of strain results

The deformations during the tests on the beams were measured in the GFRP sheet and in the concrete, [Figure 11](#) shows the beams with the strain gages installed, [Figure 11\(a\)](#) being VGR 100, [Figure 11\(b\)](#) VGR 175 and [Figure 11\(c\)](#) VGR 400.

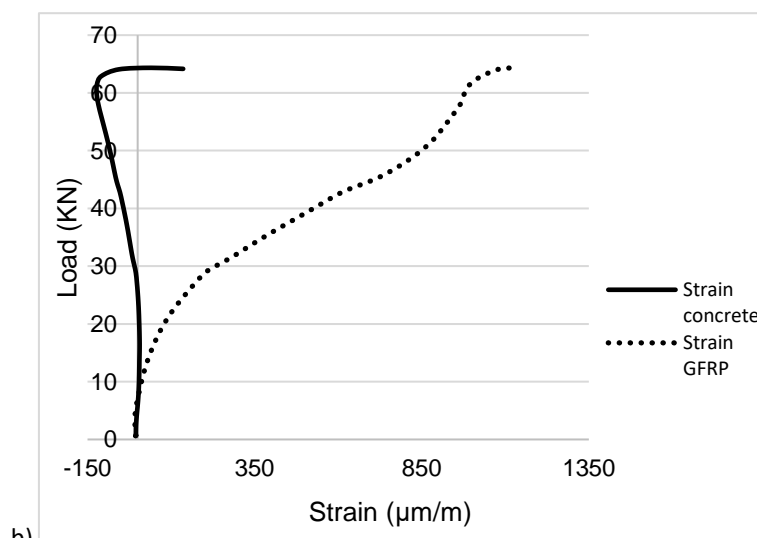


**Figure 11:** Positioning of the strain gages on the beams: a) VGR 100; b) VGR 175 and c) VGR 400

[Figure 12](#) demonstrates the graphs showing the strain analysis for the strain gages positioned on the beams and the pultruded sheet, [Figure 12\(a\)](#) being VGR 100, [Figure 12\(b\)](#) VGR 175 and [Figure 12\(c\)](#) VGR 400.



a)



b)

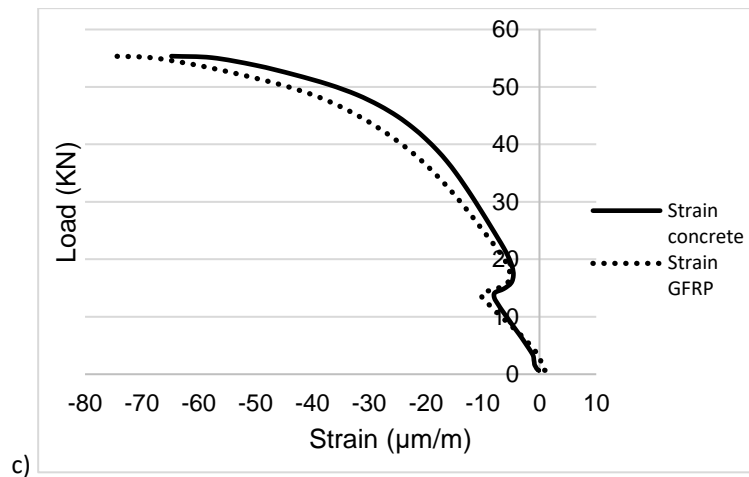


Figure 12: Graph load x strain (a) VGR 100; (b) VGR 175 and (c) VGR 400

Based on Figure 12(a), the beams of the VGR 100 group presented tensile force in the GFRP sheet, while in the beam the strains were of compression, which demonstrates the reaction of the beam to the stress acting on the strengthening.

In the beams of the group VGR 175, the deformations in the strengthening show that there was a greater solicitation of the sheet, due to a smaller number in the requested region. In the results it is also observed that the deformations presented were lower than the limit deformation of the material ( $\epsilon_{fu} = 11000 \mu\text{m/m}$ ), fact that can be related to the position of the strengthening plate in relation to the location of the cracks, being the efforts concentrated in the location of the crack and this way the strengthening was not demanded to its maximum capacity of resistance.

For the group of beams VGR 400 the strains in the beam and in the strengthening behaved similar, both presented negative strains. It is evident that the position of the plate positioned near the support, the stress generated in it was compression transmitted by the reaction of the support on the concrete. In this way it is verified not to have been requested to the efforts of the shear region, for being positioned close to the support.

#### 4. Conclusions

The strengthening with GFRP sheets was satisfactory once the load increment was positive in two groups of beams the VGR 100 and the beams of VGR 175 group.

In terms of load increase, the beams of group VGR 100 in average, was the one that presented the best result with 18,3%, however the beams of group VGR 175 obtained results very close to those obtained before strengthening, presenting an average increase of 3,6%.

The beams of VGR 400 group were the ones that obtained a load loss of 11,0%.

Regarding the vertical displacement, the beams of VGR 175 group showed better results, causing an increase of ductility in the beams.

The results of the deformations in the strengthening plate were lower than the limit deformation of the material, fact that can be related to the position of the strengthening plate in relation to the location of the cracks, being the efforts concentrated in the location of the crack and this way the strengthening was not demanded until its maximum capacity of resistance.

#### References

ABNT. 1998. *Concreto - Determinação da consistência pelo abatimento do tronco de cone*. NBR NM 67. Associação Brasileira de Normas Técnicas.

- . 2011. *Concreto e argamassa - Determinação da resistência à tração por compressão diametral de corpos de prova cilíndricos*. NBR 7222. Associação Brasileira de Normas Técnicas.
- . 2014. *Projeto de estruturas de concreto - Procedimento*. NBR 6118. Associação Brasileira de Normas Técnicas.
- . 2015. *Concreto - Procedimento para moldagem e cura de corpos de prova*. NBR 5738. Associação Brasileira de Normas Técnicas.
- . 2017. *Concreto - Determinação do módulo estático de elasticidade a compressão*. NBR 8522. Associação Brasileira de Normas Técnicas.
- Adhikary, B. B., and H. Mutsuyoshi. 2004. "Behavior of concrete beams strengthened in shear with carbon-fiber sheets". *Journal of Composites for Construction* 8, no. 3: 258-64. [https://doi.org/10.1061/\(ASCE\)1090-0268\(2004\)8:3\(258\)](https://doi.org/10.1061/(ASCE)1090-0268(2004)8:3(258)).
- Akroush, N., T. Almahallawi, M. Seif, and E. Y. Sayed-Ahmed. 2017. "CFRP shear strengthening of reinforced concrete beams in zones of combined shear and normal stresses". *Composite Structures* 162: 47-53. <https://doi.org/10.1016/j.compstruct.2016.11.075>.
- American Concrete Institute. 2005. *Building code requirements for structural concrete and commentary*. ACI 318-05. American Concrete Institute.
- . 2015. *Guide for the design and construction of externally bonded FRP systems for strengthening concrete structures*. ACI 440.2R-08. American Concrete Institute.
- Araújo, J. M. de. 2014. *Curso de Concreto Armado*. Vol. 2. Editora Dunas.
- Ary, M. I., and T. H. K. Kang. 2012. "Shear-strengthening of reinforced & prestressed concrete beams using FRP: Part I - Review of previous research". *International Journal of Concrete Structures and Materials* 6, no. 1: 41-47. <https://doi.org/10.1007/s40069-012-0004-1>.
- Baggio, D., K. Soudki, and M. Noël. 2014. "Strengthening of shear critical RC beams with various FRP systems". *Construction and Building Materials* 66: 634-44. <https://doi.org/10.1016/j.conbuildmat.2014.05.097>.
- Bielak, J., J. Schöneberg, M. Classen, and J. Hegger. 2022. "Shear capacity of continuous concrete slabs with CFRP reinforcement". *Construction and Building Materials* 320. <https://doi.org/10.1016/j.conbuildmat.2021.126117>.
- Chemrouk, M. 2015. "The deteriorations of reinforced concrete and the option of high performances reinforced concrete". *Procedia Engineering* 125: 713-24. <https://doi.org/10.1016/j.proeng.2015.11.112>.
- Chen, G. M., S. W. Li, D. Fernando, P. C. Liu, and J. F. Chen. 2017. "Full-range FRP failure behaviour in RC beams shear-strengthened with FRP wraps". *International Journal of Solids and Structures* 125: 1-21. <https://doi.org/10.1016/j.ijsolstr.2017.07.019>.
- Chen, J. F., and J. G. Teng. 2003. "Shear capacity of FRP-strengthened RC beams: FRP debonding". *Construction and Building Materials* 17, no. 1: 27-41. [https://doi.org/10.1016/S0950-0618\(02\)00091-0](https://doi.org/10.1016/S0950-0618(02)00091-0).
- Ebead, U., and H. Saeed. 2017. "FRP/stirrups interaction of shear-strengthened beams". *Materials and Structures/Materiaux et Constructions* 50, no. 2: Article number 103. <https://doi.org/10.1617/s11527-016-0973-7>.
- Hadigheh, S. A., and S. Kashi. 2018. "Effectiveness of vacuum consolidation in bonding fibre reinforced polymer (FRP) composites onto concrete surfaces". *Construction and Building Materials* 187: 854-64. <https://doi.org/10.1016/j.conbuildmat.2018.07.200>.

- Hoffman, I. S., J. H. Piva, A. Wanderlind, and E. G. P. Antunes. 2020. "Reinforced concrete beams coated with fiberglass-reinforced polymeric profiles as partial substitutes for the transverse reinforcement". *Revista IBRACON de Estruturas e Materiais* 13, no. 6: Article number e13608. <https://doi.org/10.1590/s1983-41952020000600008>.
- Hussein, M., H. M. E. D. Afefy, and A. H. A. K. Khalil. 2013. "Innovative repair technique for RC beams predamaged in shear". *Journal of Composites for Construction* 17, no. 6: Article number 04013005. [https://doi.org/10.1061/\(ASCE\)CC.1943-5614.0000404](https://doi.org/10.1061/(ASCE)CC.1943-5614.0000404).
- Kalfat, R., J. Gadd, R. Al-Mahaidi, and S. T. Smith. 2018. "An efficiency framework for anchorage devices used to enhance the performance of FRP strengthened RC members". *Construction and Building Materials* 191: 354-75. <https://doi.org/10.1016/j.conbuildmat.2018.10.022>.
- Khalifa, A., W. J. Gold, A. Nanni, and M. I. Abdel Aziz. 1998. "Contribution of externally bonded FRP to shear capacity of RC flexural members". *Journal of Composites for Construction* 2, no. 4: 195-202. [https://doi.org/10.1061/\(ASCE\)1090-0268\(1998\)2:4\(195\)](https://doi.org/10.1061/(ASCE)1090-0268(1998)2:4(195)).
- Khalifa, A., and A. Nanni. 2002. "Rehabilitation of rectangular simply supported RC beams with shear deficiencies using CFRP composites". *Construction and Building Materials* 16, no. 3: 135-46. [https://doi.org/10.1016/S0950-0618\(02\)00002-8](https://doi.org/10.1016/S0950-0618(02)00002-8).
- Koaik, A., S. Bel, and B. Jurkiewicz. 2017. "Experimental tests and analytical model of concrete-GFRP hybrid beams under flexure". *Composite Structures* 180: 192-210. <https://doi.org/10.1016/j.compstruct.2017.07.059>.
- Mugahed Amran, Y. H., R. Alyousef, R. S. M. Rashid, H. Alabduljabbar, and C. C. Hung. 2018. "Properties and applications of FRP in strengthening RC structures: A review". *Structures* 16: 208-38. <https://doi.org/10.1016/j.istruc.2018.09.008>.
- Mugahed Amran, Y. H., M. El-Zeadani, M. R. Raizal Saifulnaz, R. Alyousef, H. Alabduljabbar, F. Alrshoudi, and A. Alaskar. 2020. "RC beam strengthening using hinge and anchorage approach". *Results in Materials* 5: Article number 100047. <https://doi.org/10.1016/j.rinma.2019.100047>.
- Panda, K. C., S. K. Bhattacharyya, and S. V. Barai. 2011. "Shear strengthening of RC T-beams with externally side bonded GFRP sheet". *Journal of Reinforced Plastics and Composites* 30, no. 13: 1139-54. <https://doi.org/10.1177/0731684411417202>.
- Pellegrino, C., and C. Modena. 2006. "Fiber-reinforced polymer shear strengthening of reinforced concrete beams: Experimental study and analytical modeling". *ACI Structural Journal* 103, no. 5: 720-28. <https://doi.org/10.14359/16924>.
- Siddika, A., M. A. A. Mamun, R. Alyousef, and Y. H. M. Amran. 2019. "Strengthening of reinforced concrete beams by using fiber-reinforced polymer composites: A review". *Journal of Building Engineering* 25: Article number 100798. <https://doi.org/10.1016/j.jobbe.2019.100798>.
- Siddika, A., M. A. A. Mamun, W. Ferdous, and R. Alyousef. 2020. "Performances, challenges and opportunities in strengthening reinforced concrete structures by using FRPs – A state-of-the-art review". *Engineering Failure Analysis* 111: Article number 104480. <https://doi.org/10.1016/j.engfailanal.2020.104480>.
- Sim, J., G. Kim, C. Park, and M. Ju. 2005. "Shear strengthening effects with varying types of FRP materials and strengthening methods". *American Concrete Institute, ACI Special Publication SP-230*: 1665-79.



- Singh, S. B. 2013. "Shear response and design of RC beams strengthened using CFRP laminates". *International Journal of Advanced Structural Engineering* 5, no. 1: Article number 16. <https://doi.org/10.1186/2008-6695-5-16>.
- Triantafillou, T. C., and C. P. Antonopoulos. 2000. "Design of concrete flexural members strengthened in shear with FRP". *Journal of Composites for Construction* 4, no. 4: 198-205. [https://doi.org/10.1061/\(ASCE\)1090-0268\(2000\)4:4\(198\)](https://doi.org/10.1061/(ASCE)1090-0268(2000)4:4(198)).
- Zhang, L., W. Liu, L. Wang, and Z. Ling. 2019. "Mechanical behavior and damage monitoring of pultruded wood-cored GFRP sandwich components". *Composite Structures* 215: 502-20. <https://doi.org/10.1016/j.compstruct.2019.02.084>.
- . 2020. "On-axis and off-axis compressive behavior of pultruded GFRP composites at elevated temperatures". *Composite Structures* 236: Article number 111891. <https://doi.org/10.1016/j.compstruct.2020.111891>.